Electronic Supporting Information

Hybrid organic–inorganic supramolecular system based on a pyridine end-decorated molybdenum(II) halide cluster and zinc(II) porphyrinate

Marina V. Volostnykh,[a] Maxim A. Mikhaylov,[bc] Anna. A. Sinelshchikova,[a] Gayane A. Kirakosyan,[ad] Alexander G. Martynov,[a] Mikhail S. Grigoriev,[a] Dmitry A. Piryazev,[bc] Aslan Yu. Tsivadze,[ad] Maxim N. Sokolov[bc*] and Yulia G. Gorbunova[ad*]

[a] Frumkin Institute of Physical Chemistry and Electrochemistry, Russian Academy of Sciences, Leninsky pr. 31-4, Moscow, 119071, Russia.

[b] Nikolaev Institute of Inorganic Chemistry, Siberian Branch of the Russian Academy of Sciences, Novosibirsk 630090, Russia.

[c] Novosibirsk State University, Novosibirsk 630090, Russia.

[d] Kurnakov Institute of General and Inorganic Chemistry, Russian Academy of Sciences, Leninsky pr. 31, Moscow, 119991, Russia.

Email: yulia@igic.ras.ru

Table of contents

1. Characterization of $(Bu_4N)_2[\{Mo_6I_8\}(OOC\text{-}C_5H_4N)_6]$ (PyMoC)

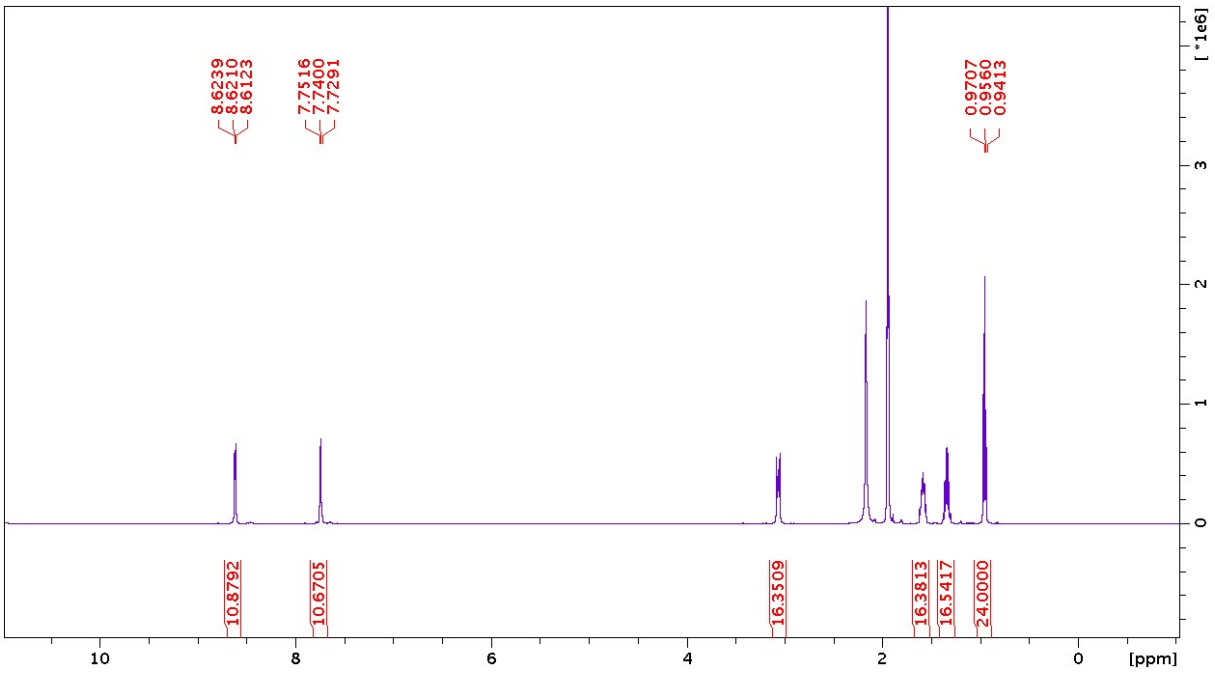

Fig. S1 ^{1}H NMR spectra (C_3D_6O, 25°C) of $(Bu_4N)_2[\{Mo_6I_8\}(OOC\text{-}C_5H_4N)_6]$.

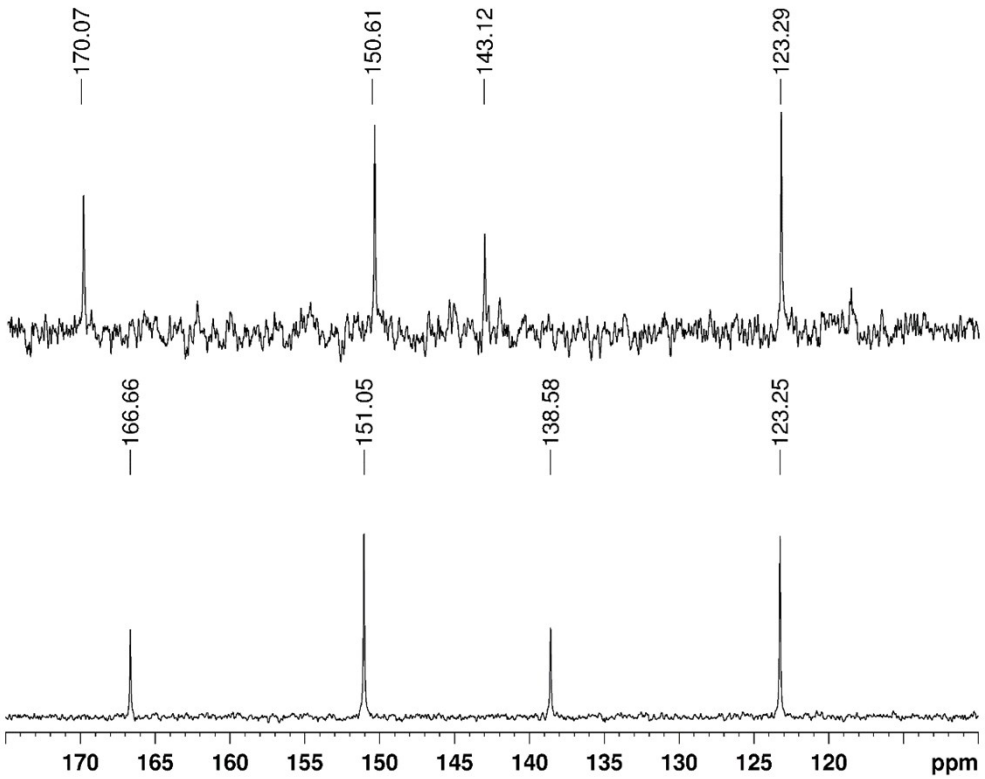

Fig. S2 ^{13}C NMR spectra (C_3D_6O, 25°C) of $(Bu_4N)_2[\{Mo_6I_8\}(OOC\text{-}C_5H_4N)_6]$ (above) and free isonicotinic acid (bottom).

2. X-ray structural analysis

2.1. XRD of PyMoC

Table S1 Crystal data and structure refinement for $(Bu_4N)_2[\{Mo_6I_8\}(OOC\text{-}C_5H_4N)_6]$

CCDC deposition code	1834666
Empirical formula	$C_{34}H_{48}N_4O_6Mo_3I_4$
FW	1404.18
Temperature, K	150.0(2)
Crystal system	triclinic
Space group	P-1
a, Å	10.5010(8)
b,Å	13.9062(11)
c,Å	16.2223(13)
α, °	113.400(2)
β, °	93.501(2)
γ, °	97.357(2)
Volume, Å^3	2139.8(3)
Z	2
ρ_{calc} g/cm^3	2.179
μ, mm^{-1}	3.796
F(000)	1332.0
Crystal size, mm^3	0.364 × 0.162 × 0.126
Radiation	MoKα (λ = 0.71073)
2Θ range for data collection, °	3.236 to 66.038
Index ranges	$-15 \le h \le 15$, $-21 \le k \le 13$, $-17 \le l \le 24$
Reflections collected	36120
Independent reflections	14578 [R_{int} = 0.0203, R_{sigma} = 0.0255]
Data/restraints/parameters	14578/0/464
Goodness-of-fit on F^2	1.038
Final R indexes [I>=2σ (I)]	R_1 = 0.0347, wR_2 = 0.0842
Final R indexes [all data]	R_1 = 0.0469, wR_2 = 0.0923
Largest diff. peak/hole, e Å^{-3}	4.15/-2.01

Table S2 Selected bond distances (Å) in $(Bu_4N)_2[\{Mo_6I_8\}(OOC\text{-}C_5H_4N)_6]$.

I(1)	Mo(1)	2.7630(4)
I(1)	Mo(2)	2.7826(4)
I(1)	Mo(3)^1	2.7742(4)
I(2)	Mo(1)	2.7689(4)
I(2)	Mo(2)	2.7901(4)
I(2)	Mo(3)	2.7857(4)
I(3)	Mo(1)	2.7633(4)
I(3)	Mo(2)^1	2.7765(4)
I(3)	Mo(3)	2.7716(4)

I(4)	Mo(1)	2.8046(4)
I(4)	Mo(2)[1]	2.7930(4)
I(4)	Mo(3)[1]	2.8067(4)
Mo(1)	Mo(2)[1]	2.6652(4)
Mo(1)	Mo(2)	2.6743(4)
Mo(1)	Mo(3)	2.6676(4)
Mo(1)	Mo(3)[1]	2.6737(4)
Mo(1)	O(1A)	2.119(3)
Mo(2)	I(3)[1]	2.7765(4)
Mo(2)	I(4)[1]	2.7929(4)
Mo(2)	Mo(1)[1]	2.6652(4)
Mo(2)	Mo(3)	2.6698(4)
Mo(2)	Mo(3)[1]	2.6719(4)
Mo(2)	O(1B)	2.168(3)
Mo(3)	I(1)[1]	2.7742(4)
Mo(3)	I(4)[1]	2.8067(4)
Mo(3)	Mo(1)[1]	2.6738(4)
Mo(3)	Mo(2)[1]	2.6719(4)
Mo(3)	O(1C)	2.144(2)

[1]1-X,-Y,-Z

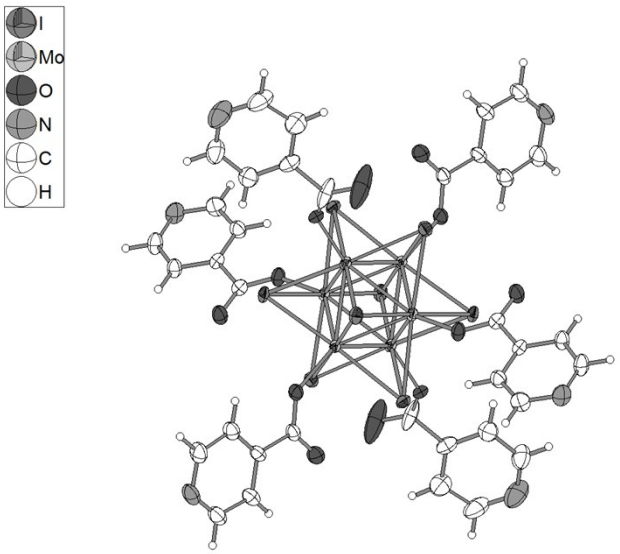

Fig. S3 Cluster anion $[\{Mo_6I_8\}(OOC\text{-}C_5H_4N)_6]^{2-}$, ellipsoids at 50% probability level.

2.2. XRD of ZnDTolP

Table S3 Crystal data and structure refinement for **ZnDTolP**

CCDC deposition code	1843802
Empirical formula	$C_{34}H_{24}N_4Zn$
FW	553.94
Temperature, K	100.15
Crystal system	monoclinic

Space group	$P2_1/c$
a, Å	14.9605(15)
b,Å	9.7595(11)
c,Å	8.5421(9)
α, °	90
β, °	93.363(6)
γ, °	90
Volume, $Å^3$	1245.1(2)
Z	2
ρ_{calc} g/cm^3	1.478
μ, mm^{-1}	1.019
F(000)	572.0
Crystal size, mm^3	0.5 × 0.5 × 0.05
Radiation	MoKα (λ = 0.71073)
2Θ range for data collection, °	8.186 to 56.09
Index ranges	-19 ≤ h ≤ 19, -12 ≤ k ≤ 12, -10 ≤ l ≤ 11
Reflections collected	12363
Independent reflections	2980 [R_{int} = 0.0757, R_{sigma} = 0.0709]
Data/restraints/parameters	2980/90/181
Goodness-of-fit on F^2	1.074
Final R indexes [I>=2σ (I)]	R_1 = 0.0713, wR_2 = 0.1641
Final R indexes [all data]	R_1 = 0.0920, wR_2 = 0.1751
Largest diff. peak/hole, e $Å^{-3}$	1.24/-0.76

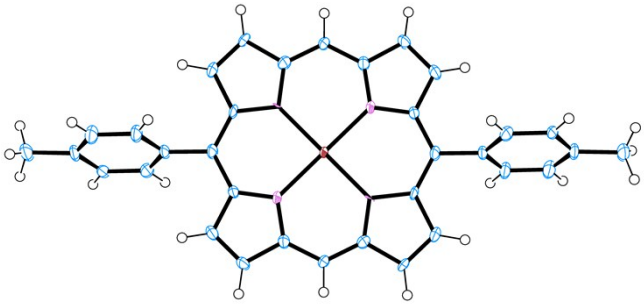

Fig. S4 ORTEP drawing of **ZnDTolP**. Thermal ellipsoids are at the 50% probability level.

Table S4 Selected bond distances (Å) in **ZnDTolP**.

Zn1	N1	2.032(4)
Zn1	$N1^1$	2.032(4)
Zn1	$N2^1$	2.011(4)
Zn1	N2	2.011(4)
N1	C1	1.369(6)
N1	C4	1.378(6)
N2	C6	1.374(6)

N2	C9	1.411(6)
C1	C2	1.436(7)
C1	C10[1]	1.418(7)
C2	C3	1.354(8)
C3	C4	1.441(7)
C4	C5	1.386(7)
C5	C6	1.387(7)
C6	C7	1.441(7)
C7	C8	1.363(7)
C8	C9	1.451(7)
C9	C10	1.403(7)
C10	C1[1]	1.418(7)
C10	C11	1.488(7)
C11	C12	1.390(9)
C11	C16	1.390(9)
C12	C13	1.389(7)
C13	C14	1.396(10)
C14	C15	1.391(10)
C14	C17	1.523(8)
C15	C16	1.399(7)

[1]1-x,1-y,-z

2.3. XRD of CP_2 and CP_6

Table S5 Crystal data and structure refinement for **CP_2** and **CP_6.**

Parameter	**CP_2**	**CP_6_sq**
CCDC deposition code	1843800	1843801
Chemical formula	$C_{140}H_{152}Cl_8I_8Mo_6N_{16}O_{12}Zn_2$	$C_{368}H_{356}Cl_8I_8Mo_6N_{40}O_{14}Zn_8$
Chemical formula moiety	$C_{104}H_{72}I_8Mo_6N_{14}O_{12}Zn_2$, $2(C_{16}H_{36}N)$, $4(CH_2Cl_2)$	$C_{240}H_{168}I_8Mo_6N_{30}O_{12}Zn_6$, $2(C_{34}H_{26}N_4OZn)$, $2(C_{16}H_{36}N)$, $4(CH_2Cl_2)$, $4(C_6H_{14})$
FW	4255.95	7960.31
Temperature, K	100(2)	100(2)
Crystal system, space group	Monoclinic, $P2_1/c$	Triclinic, P-1
Unit cell dimensions a, b, c, Å	11.9029(7), 21.0461(13), 29.4339(19)	20.2530(10), 20.5959(11), 21.6995(10)
α, β, γ, °	90, 91.286(3), 90	103.620(2), 107.057(3), 98.424(2)
Volume, Å^3	7371.6(8)	8180.5(7)
Z	2	1
Density (calculated), g/cm^3	1.917	1.616
μ, mm^{-1}	2.697	1.685
Crystal size, mm	0.4 × 0.2 × 0.08	0.4 × 0.2 × 0.06
Radiation, λ, Å	MoKα, 0.71073	MoKα, 0.71073
Data collection range, θ, °	4.082 – 27.499	4.085 – 27.499

Index ranges	$-15 \le h \le 14, -27 \le k \le 27, -38 \le l \le 37$	$-26 \le h \le 26, -26 \le k \le 26, -28 \le l \le 28$
Reflections collected	66689	62272
Unique reflections/R_{int}	16876/0.0392	28666/0.1055
Reflections with $I > 2\sigma(I)$	13166	12659
Data/restraints/parameters	16876/0/871	28666/1402/1932
Goodness-of-fit on F^2	1.021	0.941
Weight scheme	$w = 1/[\sigma^2(F_o^2) + (0.0260P)^2 + 25.6363P]$ where $P=(F_o^2+2F_c^2)/3$	$w = 1/[\sigma^2(F_o^2) + (0.1179P)^2]$ where $P=(F_o^2+2F_c^2)/3$
Final R indexes [$I>=2\sigma(I)$]	$R_1 = 0.0320$, $wR_2 = 0.0681$	$R_1 = 0.0717$, $wR_2 = 0.1719$
Final R indexes [all data]	$R_1 = 0.0510$, $wR_2 = 0.0777$	$R_1 = 0.1936$, $wR_2 = 0.2503$
Largest diff. peak/ hole, e/Å3	3.14/-1.98	2.76/-1.61

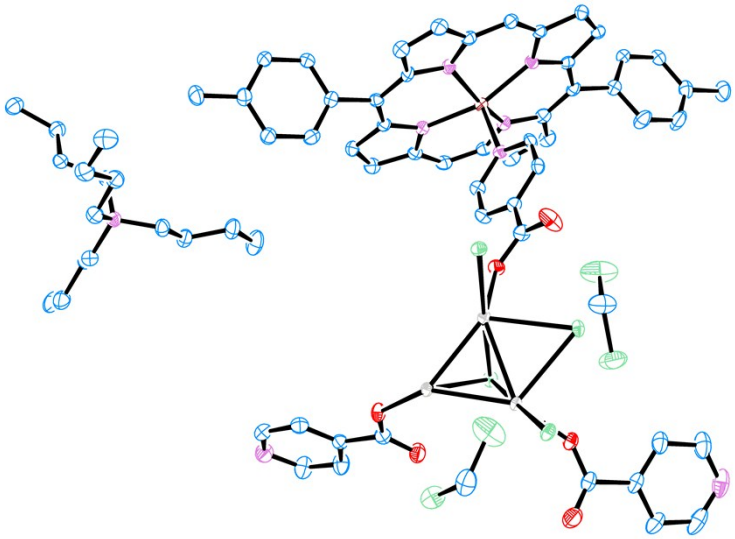

Fig. S5 ORTEP drawing of asymmetric unit of **CP_2**. Thermal ellipsoids are at the 50% probability level. Hydrogen atoms are omitted for clarity. C atoms are marked by blue, N by magenta, O by red, Cl and I by green, Zn by dark-red, Mo by grey.

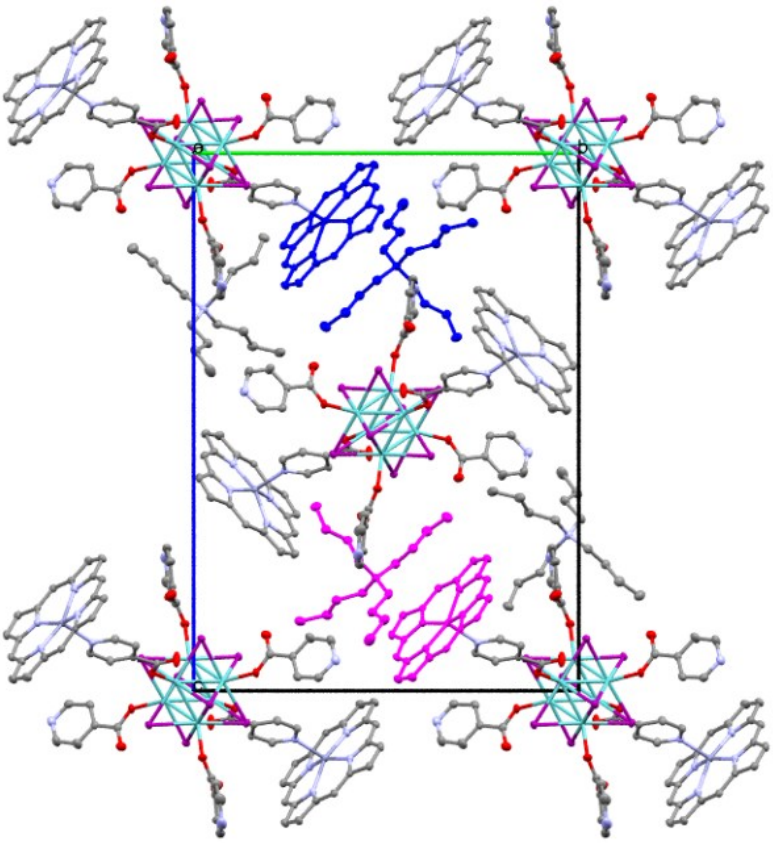

Fig. S6 Packing of **CP_2**. Hydrogen atoms and solvent molecules CH_2Cl_2 are omitted for clarity. Ellipsoids are at the 50% probability level.

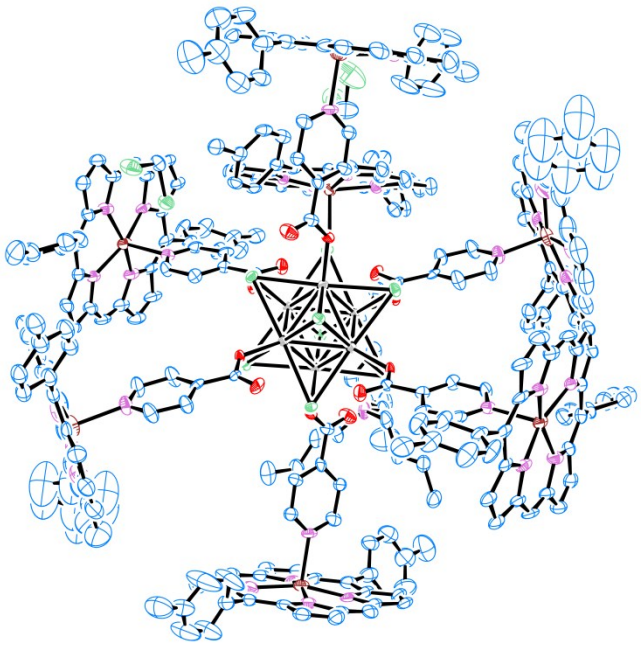

Fig. S7 ORTEP drawing of **CP_6**. Thermal ellipsoids are at the 30% probability level. Hydrogen atoms are omitted for clarity. C atoms are marked by blue, N by magenta, O by red, Cl and I by green, Zn by dark-red, Mo by grey.

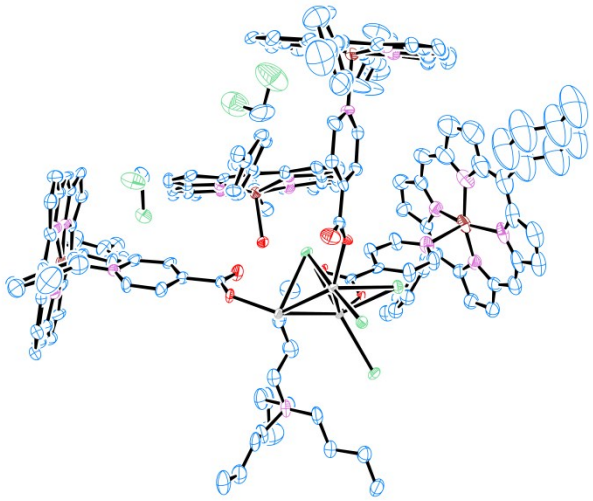

Fig. S8 ORTEP drawing of asymmetric unit of **CP$_6$**. Thermal ellipsoids are at the 30% probability level. Hydrogen atoms are omitted for clarity. C atoms are marked by blue, N by magenta, O by red, Cl and I by green, Zn by dark-red, Mo by grey.

Table S6 Geometry of Mo cluster complexes.

Complex	Mo–Mo	Mo–μ_3–I	Mo–L	Ref
[{Mo$_6$(μ_3-I)$_8$}*L*$_6$]$^{2-}$	2.6599(7)–2.6725(8)	2.7642(7)–2.8057(7)	*L* = C6H5COO; 2.097(4)	[1]
PyMoC	2.6652(4)–2.6738(4)	2.7630(4)–2.8067(4)	*L* = C5NH4COO; 2.119(3)–2.168(3)	This work
CP$_2$	2.6570(5)–2.6774(5)	2.7728(5)–2.7937(5)	*L* = C5NH4COO; 2.110(3)–2.136(3)	This work
CP$_6$	2.6625(14)–2.6707(16)	2.7570(13)–2.8031(14)	*L* = C5NH4COO; 2.092(8)–2.102(8)	This work

Table S7 Selected bond lengths (Å) and angles (°) for the hybrid supramolecular complexes **CP$_n$.**

	Zn–N(por), Å	Zn–N(py), Å	Zn–N$_4$ deviation, Å	Maximum C$_\beta$ deviation from N$_4$, Å	Dihedral angles N$_4$/N$_4$[2],°	Dihedral angles C$_6$H$_4$(tolyl)/N$_4$,°
CP$_2$	Zn1–N14 2.073(3) Zn1–N13 2.070(3) Zn1–N12 2.086(3) Zn1–N15 2.074(3)	Zn1–N11 2.155(3)	Zn1 0.383(2)	C103 -0.206(7) C108 0.137(7) C120 0.203(7) C124 0.278(7)		60.8 78.0
CP$_6$_sq	Zn11–N14 2.045(14) Zn11–N12 2.062(15) Zn11–N13 2.097(13)	Zn11–N11 2.137(11)	Zn11 0.293(6)	C102 0.233(25) C108 0.050(25) C119 0.251(23) C124 -0.121(25)	85.4 (por 1-2) 47.7 (por 1-3)	80.6 60.6

	Zn11–N15 2.074(13) Zn21–N25 2.051(16) Zn21–N23 2.043(14) Zn21–N22 2.036(15) Zn21–N24 2.068(16) Zn31–N34 2.073(18) Zn31–N32 2.044(15) Zn31–N33 2.037(17) Zn31–N35 2.057(15)	 Zn21–N21 2.136(11) Zn31–N31 2.152(13)	 Zn21 0.282(7) Zn31 0.312(8)	 C202 -0.151(25) C208 -0.008(26) C219 0.030(31) C225 -0.042(27) C302 0.114(30) C307 -0.236(33) C319 0.154(51) C325 -0.065(30)	63.3 (por 2-3)	 72.1 68.6 69.6 61.8
CP_6_sq Zn porphyrin not bonded with cluster	Zn41–N43 2.055(12) Zn41–N42 2.064(11) Zn41–N41 2.084(13) Zn41–N44 2.085(12)	Zn41– O41[1] 2.081(8)	Zn41 0.348(6)	C402 0.113(27) C408 0.058(23) C419 0.177(23) C425 0.230(23)		58.3 66.2

[1] H_2O molecule axially coordinated to Zn(II) porphyrin not bonded with cluster

[2] Dihedral angles between symmetrically independent porphyrin molecules.

3. Powder X-ray diffraction analysis (PXRD)

a)

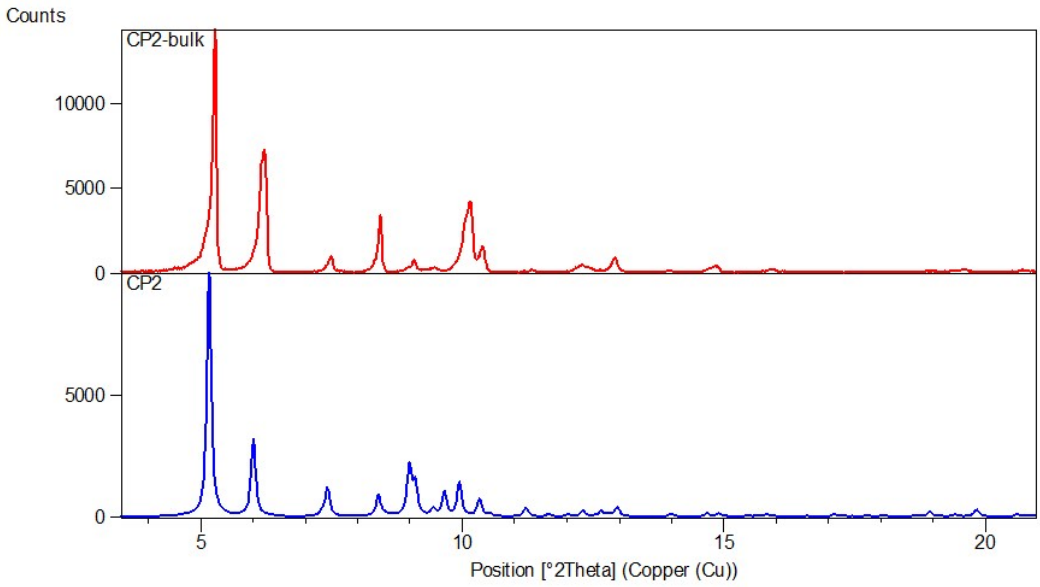

b)

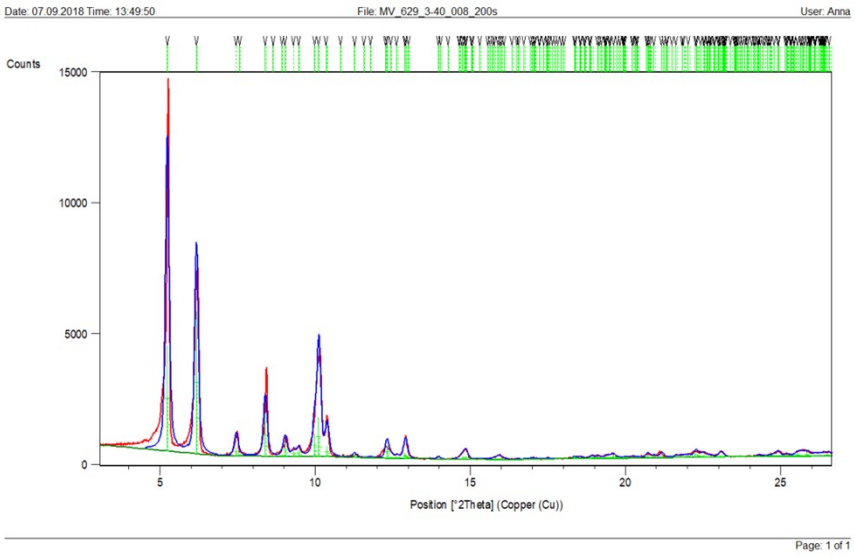

Fig. S9 PXRD pattern of **CP_2-bulk** a) Comparison of PXRD pattern of **CP_2-bulk** (red) with theoretical powder pattern calculated in Mercury from single crystal data for **CP_2** (blue), b) The result of the Le-bail fit of **CP_2-bulk**.

a)

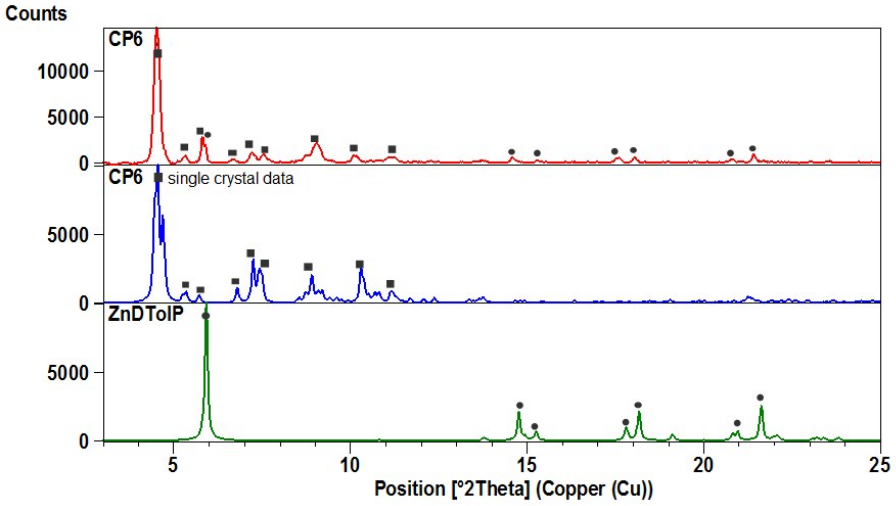

b)

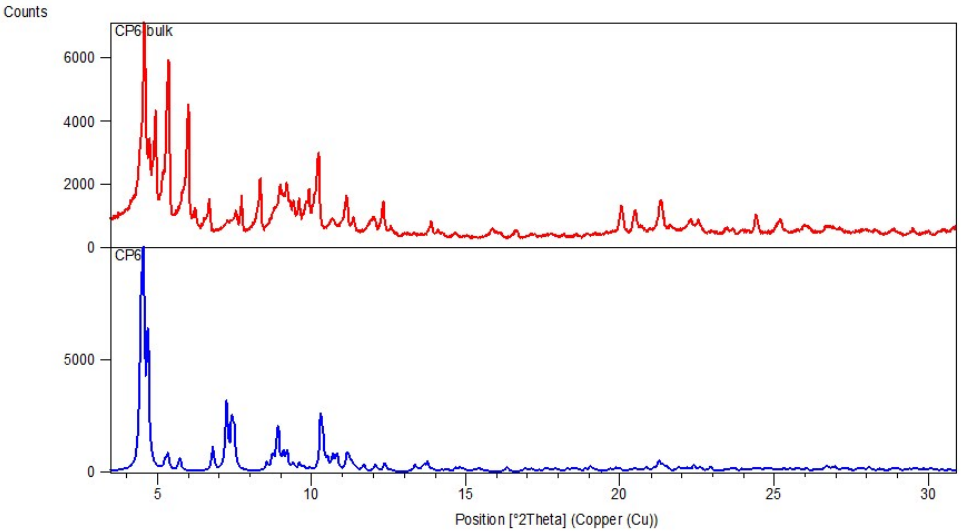

Fig. S10 PXRD pattern of **CP_6**. a) PXRD pattern of **CP_6** sample from single crystal synthesis (red) compared with theoretical powder pattern for **CP_6** single crystal data (blue) and theoretical powder pattern for **ZnDTolP** single crystal (green), b) comparison of PXRD pattern of **CP_6-bulk** (red) with theoretical powder pattern calculated in Mercury from single crystal data for **CP_6** (blue). The main phase is **CP_6** but it is not pure.

4. NMR spectroscopy

4.1. DOSY Experiments

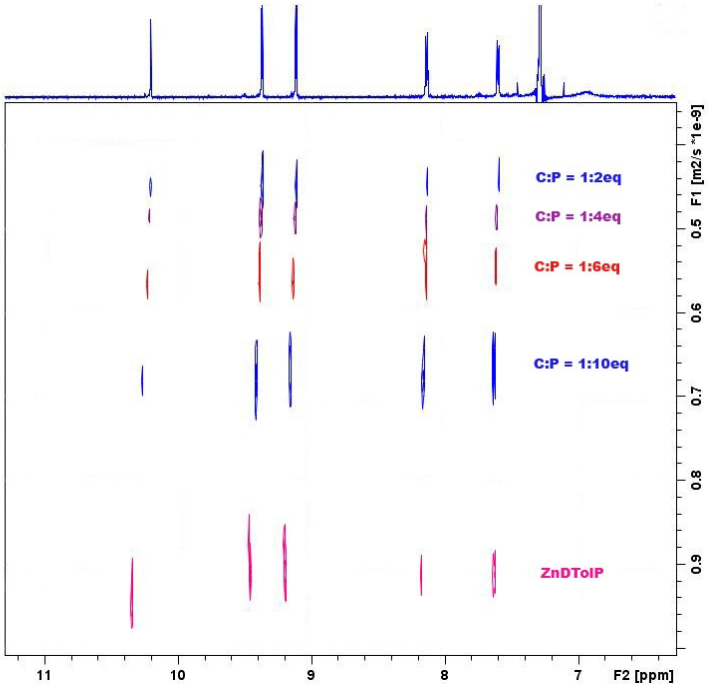

(A)

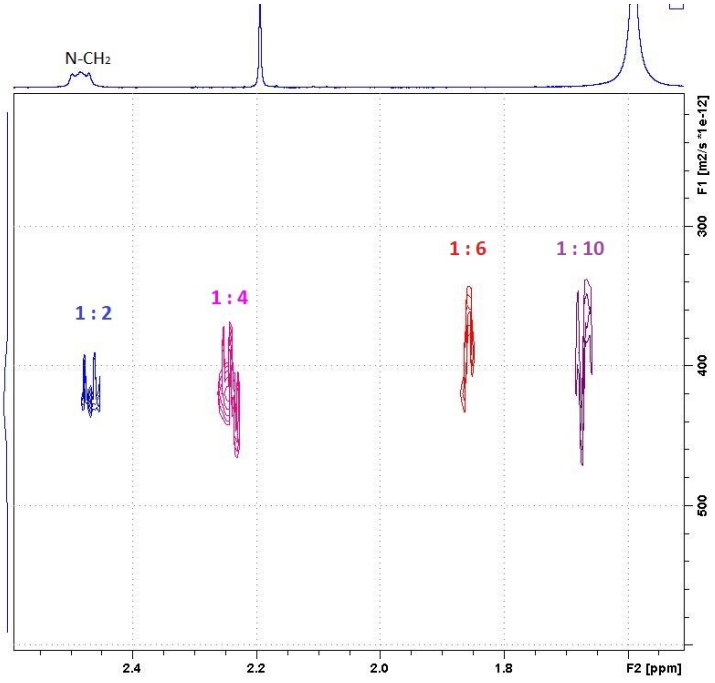

(B)

Fig. S11 DOSY ^{1}H NMR spectra (in $CDCl_3$ at 303 K) of **ZnDTolP**, **PyMoC** and their mixtures at different molar ratios (C : P = 1:2 – 1:10): (A) the porphyrin spectral range and (B) the range of the N-CH_2 group of Bu_4N^+ (see Fig. 4).

Table S8 (Left) Experimental diffusion coefficients (*Ds*) of **ZnDTolP**, **PyMoC** and their mixtures at different molar ratios (C : P = 1:2 – 1:10) according DOSY-NMR data. (Right) Changes of *Ds* at the different molar ratios (C : P = 1:2 – 1:10) in $CDCl_3$.

C:P ratio	D_s, m²/s Porph/Py*	D_s, m²/s Bu_4N^+ **
0 : 1 (ZnDTolP)	8.88×10^{-10}	
1 : 0 (PyMoC)	4.63×10^{-10}	4.65×10^{-10}
1 : 2	4.11×10^{-10}	4.11×10^{-10}
1 : 4	4.46×10^{-10}	4.05×10^{-10}
1 : 6	5.0×10^{-10}	3.84×10^{-10}
1 : 10	6.2×10^{-10}	3.83×10^{-10}

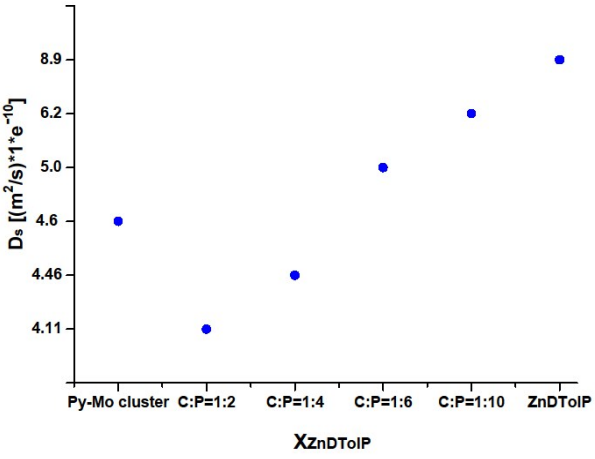

* The average of the D_s values determined for the five signal of the porphyrin core.

** The D_s value determined for the N-CH_2 signal of the Bu_4N^+ cation.

4.2. Low-temperature NMR Experiments

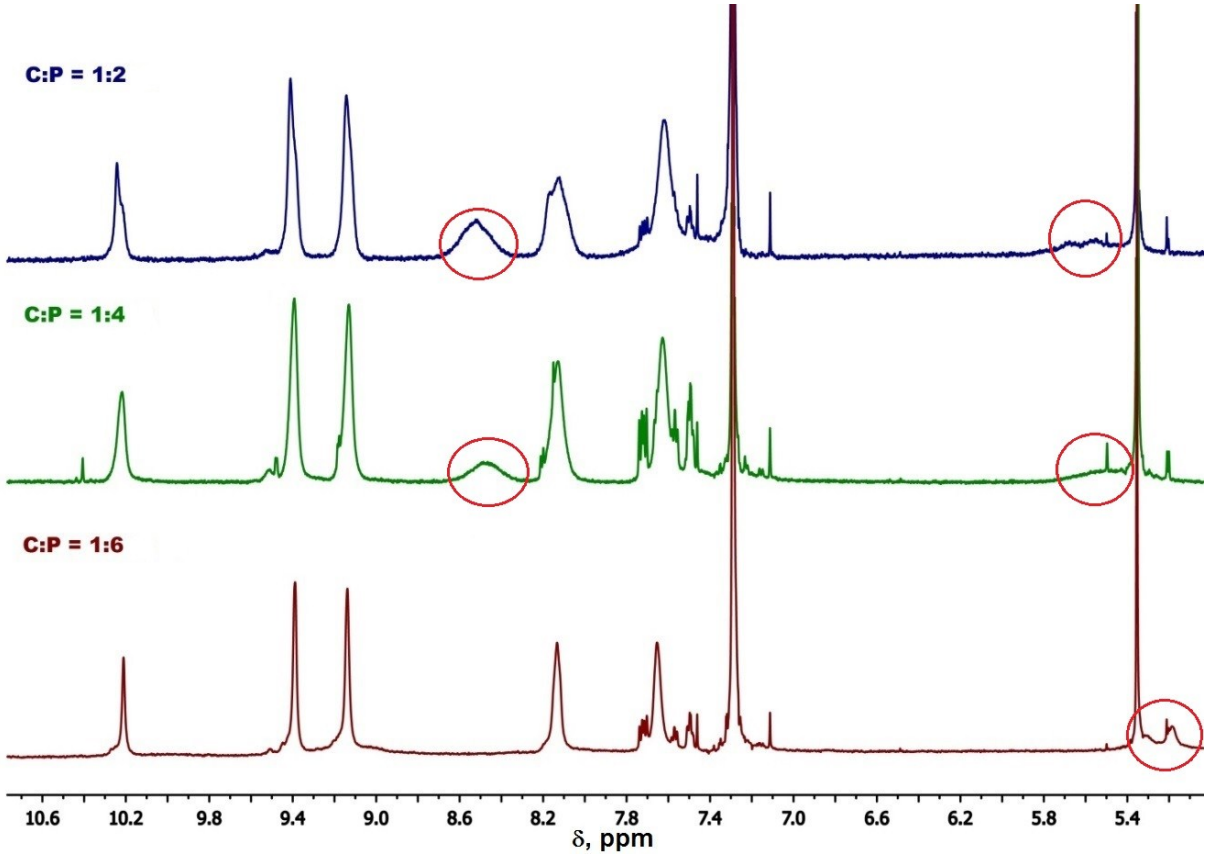

Fig. S12 Low-temperature ^1H NMR spectra (in $CDCl_3$ at 233 K) of mixtures of **ZnDTolP** and **PyMoC** at different cluster : porphyrin molar ratios (C : P = 1:2 – 1:6).

5. UV-Vis spectroscopy

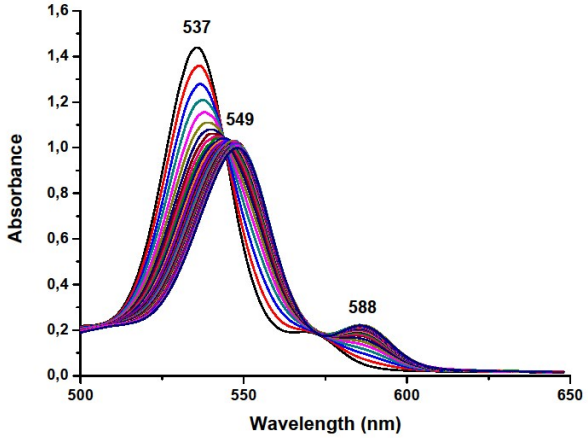

(A)

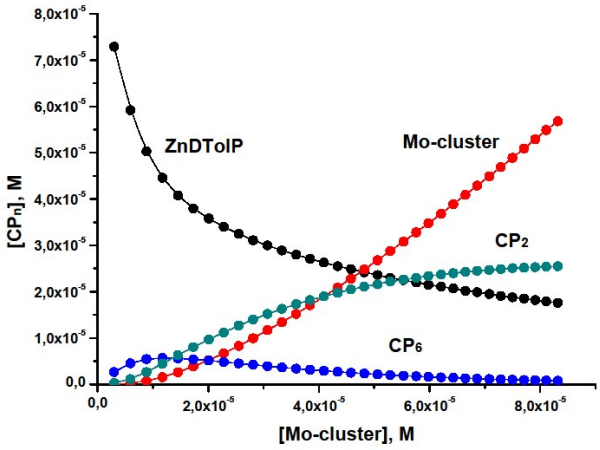

(B)

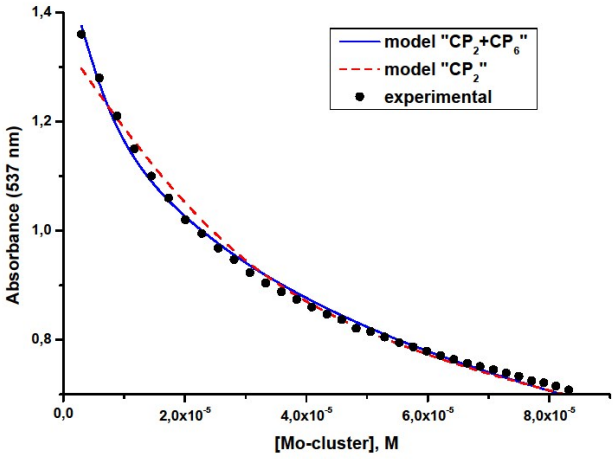

(C)

Fig. S13 (A) UV-Vis spectral changes at 298 K of **ZnDTolP** (90μM) in CH_2Cl_2 upon titration with **PyMoC** solution (0.034 equiv each addition). (B) Species concentration plot of **ZnDTolP** (black), hybrid complex **CP_2** (aquamarine) and hybrid complex **CP_6** (blue) upon the addition of **PyMoC**. (C) Absorbance changes of **ZnDTolP** at 537 nm upon the addition of **PyMoC**.